

Myricetin alleviates H₂O₂-induced senescence and apoptosis in rat nucleus pulposus-derived mesenchymal stem cells

Tian Xie, Ruijie Pan, Wenzhuo Huang, Sheng Dong, Shizhen Wu, Yuhui Ye

Department of Orthopedics, Wuhan Hospital of Traditional Chinese Medicine, Wuhan, China

Abstract

Introduction. Transplantation of mesenchymal stem cells (MSCs) has been reported to be a novel promising target for the regeneration of degenerated intervertebral discs (IVDs). However, the culture and survival limitations of MSCs remain challenging for MSC-based biological therapy. Myricetin, a common natural flavonoid, has been suggested to possess antiaging and antioxidant abilities. Therefore, we investigated the biological function of myricetin, and its related mechanisms involving cell senescence in intervertebral disc degeneration (IDD).

Material and methods. The nucleus pulposus-derived mesenchymal stem cells (NPMSCs) were isolated from 4-month-old Sprague-Dawley (SD) rats and identified by examining surface markers and multipotent differentiation. Rat NPMSCs were cultured in an MSC culture medium or culture medium with different concentrations of H₂O₂. Myricetin or the combination of myricetin and EX527 were added to the culture medium to investigate the effects of myricetin. Cell viability was evaluated by cell counting kit-8 assays (CCK-8). The apoptosis rate was determined using Annexin V/PI dual staining. The mitochondrial membrane potential (MMP) was analyzed by a fluorescence microscope after JC-1 staining. The cell senescence was determined by SA-β-Gal staining. MitoSOX green was used to selectively estimate mitochondrial reactive oxygen species (ROS). Apoptosis-associated proteins (Bax, Bcl2, and cleaved caspase-3), senescence markers (p16, p21, and p53), and SIRT1/PGC-1α signaling pathway-related proteins (SIRT1 and PGC-1α) were evaluated by western blotting.

Results. The cells isolated from nucleus pulposus (NP) tissues met the criteria for MSCs. Myricetin showed no cytotoxicity up to a concentration of 100 μM in rat NPMSCs cultured for 24 h. Myricetin pretreatment exhibited protective effects against H₂O₂-induced apoptosis. Myricetin could also alleviate H₂O₂-induced mitochondrial dysfunctions of increased mitochondrial ROS production and reduced MMP. Moreover, myricetin pretreatment delayed rat NPMSC senescence, as evidenced by decreased expression of senescence indicators. Pretreatment of NPMSCs with 10 μM EX527, a selective inhibitor of SIRT1, prior to exposure to 100 μM H₂O₂, reversed the inhibitory effects of myricetin on cell apoptosis.

Conclusions. Myricetin could affect the SIRT1/PGC-1α pathway to protect mitochondrial functions and alleviate cell senescence in H₂O₂-treated NPMSCs. (*Folia Histochemica et Cytobiologica* 2023, Vol. 61, No. 2, 98–108)

Keywords: nucleus pulposus mesenchymal stem cells; myricetin; apoptosis; cell senescence; mitochondrial membrane potential; SIRT1; ROS

Correspondence address:

Tian Xie

Department of Orthopedics, Wuhan Hospital of Traditional Chinese Medicine, Wuhan, China

e-mail: xietiandoctor@hotmail.com

Introduction

Low back pain (LBP) is a prevalent sequela of spinal conditions [1]. As the most common musculoskeletal disorder, intervertebral disc degeneration (IDD) accounts for nearly 40% of LBP etiologies [2]. Tissue weakenings from loading history, nutritional compromise, genetic inheritance, and aging are causes of IDD [3]. Approximately 90% of individuals are diagnosed with IDD when they are over 50 years old [4]. Currently, vertebrectomy, decompression, and drug therapy slightly relieve the pain [5]. In practice, however, disc degeneration of adjacent segments and recurrent pain are adverse reactions accompanying these therapies [6]. Therefore, novel effective therapeutic options for IDD treatment should be initiated.

An intervertebral disc (IVD), which consists of an inner nucleus pulposus (NP) core and outer annulus fibrosus (AF), is a gel-like structure that separates the vertebrae. IVDs allow the motion of vertebrae and distribute pressure while resisting compressive loading [7]. NP, composed of nucleus pulposus cells (NPCs) and extracellular matrix (ECM) components, plays a key role in the function of IVDs [8]. However, NPCs are characterized by poor proliferative, differentiative, and self-renewal abilities [9]. Mesenchymal stem cells (MSCs) have the potential to self-renew, proliferate, and differentiate into specific types of cells [10]. Accumulating evidence has suggested the therapeutic value of MSCs in IDD treatment [11–13]. However, for MSC-based biological therapy, culture conditions and survival limitations of MSCs remain challenging [14]. Nucleus pulposus-derived MSCs (NPMSCs) are suggested to improve IVD repair and regeneration [15–17]. Unfortunately, microenvironmental inflammation and oxidative stress can cause cell senescence and apoptosis [18]. Therefore, the investigation of approaches to protect NPMSCs from apoptosis and senescence is necessary for IDD treatment.

Overproduction of reactive oxygen species (ROS) is observed in rat degenerative discs and human NP specimens with IDD advancing [19]. A mitochondrion is the main cellular energy and also the target of ROS generation [20]. Mitochondrial membrane potential (MMP) collapse can be induced by ROS [21]. Senescence is a cellular response characterized by a stable cell cycle arrest that limits the proliferative potential of cells. During cellular senescence, levels of p16, p53, and p21 are shown to be upregulated, and inhibiting p16, p21, or p53 expression may reduce the number of senescent MSCs or restore their proliferative ability [22, 23]. The most studied mechanisms implicated in the process of MSC senescence are ROS production, DNA damage, and mitochondrial dysfunctions [24].

Hence, attenuation of ROS production and mitochondrial dysfunction is beneficial in preventing NPMSC senescence.

The silent information regulator of transcription 1 (SIRT1) is a highly conserved member of NAD⁺-dependent histone deacetylases. Apart from acting on histones and other substrates, SIRT1 deacetylates its substrate peroxisome proliferator-activated receptor Gamma Coactivator-1 α (PGC-1 α) and consequently increases PGC-1 α activity [25]. The SIRT1/PGC-1 α pathway, a classic pathway related to mitochondrial function, is reported to be involved in antiaging and antioxidant activities [26, 27].

Myricetin (3,5,7-trihydroxy-2-(3,4,5-trihydroxyphenyl)-4chromenone) is a common flavonoid compound present in tea, berries, fruits, vegetables, and medical herbs. Myricetin has been suggested to play an antioxidative role in cell membranes and mitochondria [28]. Additionally, myricetin can recover the mitochondrial impairments in N2a-SW cells [29]. Moreover, myricetin has been found to promote the activation of the SIRT1/PGC-1 α pathway in mouse skeletal muscle to enhance mitochondrial activity [30]. Therefore, this study was designed to investigate whether myricetin could improve suppressed mitochondrial function *via* the SIRT1/PGC-1 α pathway and inhibit the expression of cell senescence markers. We hypothesized that myricetin would protect NPMSCs from cell senescence. The results of our study suggest that myricetin would be a promising therapeutic option for IDD treatment.

Material and methods

Animals. Sprague-Dawley (SD) rats (male, 4 month-old; SLAC Laboratory Animal Company, Shanghai, China) were housed in a 12 h light/dark cycle at 23 \pm 2° with 50 \pm 5% humidity. All rats were given free access to food and water. The protocols for the animal care and use of the laboratory animals were approved by the Ethics Committee of Wuhan Hospital of Traditional Chinese Medicine (Wuhan, China).

Isolation of nucleus pulposus-derived mesenchymal stem cells (NPMSCs). To isolate NPMSCs, 20 SD rats were anesthetized by an overdose of sodium pentobarbital (100 mg/kg) and sacrificed. Coccygeal IVD tissues were harvested under aseptic conditions as previously described [31]. Then gel-like NP tissues were isolated under a light microscope. The isolated NP tissues were subsequently washed three times with phosphate-buffered saline (PBS) containing 1% penicillin-streptomycin (NovoBiototechnology, Beijing, China) and digested in 0.2% collagenase II (Yeasen, Shanghai, China) for 2 h at 37°. After centrifugation at 800 g for 5 min, the cell pellets were cultured in MSC medium (Cyagen, Jiangsu, China) containing 20% fetal bovine serum (FBS; Biorab, Beijing, China) and 1% penicillin/streptomycin.

Afterward, the cells were seeded into 25 cm² culture flasks with 2×10^5 cells/mL and incubated at 37° with 5% CO₂. The medium was removed twice a week. The cells were passaged at a 1:3 ratio at 80–90% confluence. The rat NPMSCs subsequently used were at passage 3.

Immunophenotypic characterization. According to the standards proposed by the International Society for Cellular Therapy (ISCT), the expression of MSC surface markers (CD73, CD90, CD105) and hematopoietic stem cell markers (CD34, CD45, HLA-DR) was determined. Briefly, 2×10^5 rat NPMSCs at passage 3 were incubated at room temperature in the dark with antibodies against HLA-DR (ab239283, 10 μL for 10⁶ cells; Abcam), CD34 (sc7324, 1 μg per 1 × 10⁶ cells; Santa Cruz Biotechnology, Santa Cruz, CA, USA), CD45 (ab33916, 1:50; Abcam), CD73 (ab282789, 0.2 μg/mL; Abcam), CD90 (ab226, 1:500; Abcam), and CD105 (sc18893, 1 μg per 1 × 10⁶ cells; Santa Cruz) for 30 min. Subsequently, the cells were washed twice with PBS and resuspended in 500 μL of PBS. The labeled cells were analyzed by flow cytometry (FACSCalibur, BD Bioscience, Franklin Lakes, NJ, USA).

Multipotent differentiation. To assess the multilineage differentiation potential of NPMSCs, osteogenic and adipogenic differentiation were induced by osteogenic and adipogenic differentiation assay kits (Cyagen) separately [32]. Briefly, harvested rat NPMSCs at passage 3 were resuspended at a density of 5×10^3 cells/mL and seeded onto six-well plates. For osteogenic differentiation, NPMSCs were cultured with osteogenic differentiation medium (medium containing 87.5% basal media, 10% FSB, 1% penicillin-streptomycin, 1% glutamine, 1% β-glycerophosphate, 0.2% ascorbate, and 0.01% dexamethasone). The medium was changed every 3 days. After 21 days of differentiation, the cells were fixed and stained with Alizarin red (Sigma-Aldrich, St-Louis, MO, USA) and then observed under an inverted microscope as described in kit instructions. For adipogenic differentiation, NPMSCs were incubated with adipogenic differentiation medium A (medium containing 87.5% basal media, 0.1% 3-isobutyl-1-methylxanthine, 1% glutamine, 1% penicillin-streptomycin, 0.1% dexamethasone, 0.1% rosiglitazone, 0.2% insulin, and 10% FBS) for 3 days. Then, medium B (medium containing 87.5% basal media, 0.2% insulin, 1.0% penicillin-streptomycin, 1.0% glutamine, and 10% FBS) was changed and incubated for 1 day. This 4-day cycle was repeated four times and then incubated with medium for 1 day. After that, the cells were fixed and stained by oil red O (Sigma-Aldrich) and then observed with an inverted microscope.

Measurements of cell viability by Cell counting kit-8 (CCK-8) assay. The cytotoxicity of H₂O₂ and the effects of myricetin on NPMSCs were detected by CCK-8 assays. Briefly, rat NPMSCs were seeded onto 96-well plates (5×10^3 cells/well) at 37° with 5% CO₂. When reaching 80–90% confluency, the cells were treated with 0–400 μM of H₂O₂ for 0–6 h or 0–100 μM of myricetin (purity 98.08%; MedChemExpress, Shanghai, China) for 0–24 h followed by addition of 10 μL of CCK-8 reagent (MedChemExpress). After 4 h of incubation, the optical den-

sity at 450 nm was estimated in a microplate reader (Bio-Rad, Hercules, CA, USA).

Cell treatment. According to the results of the CCK-8 assay, we treated rat NPMSCs with 50 μM myricetin for 24 h prior to exposure to 100 μM H₂O₂ for 6 h in the subsequent studies. To further determine whether the protective effects of myricetin were associated with SIRT1/PGC-1α activity, the rat NPMSCs were pre-conditioned with 10 μM EX527 (a selective inhibitor of SIRT1) prior to exposure to 100 μM H₂O₂ for 6 h at room temperature. Collectively, the rat NPMSCs were divided into the control, the H₂O₂, the H₂O₂ + myricetin, and the H₂O₂ + myricetin + EX527 groups. The concentration of EX527 was selected according to a previous study [33].

Cell apoptosis analysis. The rat NPMSCs were seeded onto a six-well plate (5×10^5 cells/well) and incubated with MSC culture medium at 37° with 5% CO₂. When the cells grew to 80% confluence, they were subjected to different interventions as designed. Then the cells were washed with PBS and collected by trypsinization. Finally, the rat NPMSCs were incubated with an Annexin V-FITC/PI Apoptosis Detection Kit (Research-Bio, Shanghai, China) at room temperature in the dark for 30 min, and then cell apoptosis was analyzed by flow cytometry. Apoptosis rates were calculated as the sum of early-apoptotic (Annexin V⁺/PI⁻) and late-apoptotic (Annexin V⁺/PI⁺) cells.

Western blotting. Total protein was isolated from the rat NPMSCs using Radioimmunoprecipitation Assay (RIPA) lysis buffer (Absin Biotech, Shanghai, China) with phosphatase and protease inhibitor cocktails (MedChemExpress, Shanghai, China). Protein concentration was examined using an Enhanced Bicinchoninic Acid Assay (BCA) Protein assay kit (Beyotime, Shanghai, China). Proteins (30 μg) were separated on 10% acrylamide gels using sodium dodecyl sulfate-polyacrylamide gel electrophoresis (SDS-PAGE) and subsequently transferred onto polyvinylidene fluoride (PVDF) membranes (Millipore, Shanghai, China). After 2-h blocking in 5% skimmed milk, the membranes were incubated overnight with primary antibodies against p21 (ab109199, 1:1000; Abcam, Shanghai, China), cleaved caspase-3 (#9661, 1:1000; Cell Signaling Technology, Shanghai, China), p16 (ab51243, 1:2000; Abcam), Bax (ab182733, 1:2000; Abcam), Bcl-2 (ab196495, 1:2000; Abcam), β-Actin (ab8227, 1:3000; Abcam), p53 (ab90363, 1:250; Abcam), SIRT1 (ab189494, 1:1000; Abcam) and PGC-1α (ab191838, 1:1000; Abcam) at 4°. After being washed with Tris-buffered saline three times, the membranes were incubated with secondary antibodies for 2 h at room temperature. The blots were then developed using enhanced chemiluminescence (Yeasen) and imaged using the chemiluminescence detection system (Bio-Rad). The band density was quantified using ImageJ software (National Institutes of Health, Bethesda, MD, USA). β-Actin was used as the loading control.

Determination of mitochondrial membrane potential. Mitochondrial membrane potential (MMP) was measured using the Tetraethylbenzimidazolycarbocyanine iodide (JC-1) assay (ab113850; Abcam). After PBS washing, the cells from different

groups were collected by trypsinization. Then, the cells were washed with PBS twice and suspended with 2 μ M JC-1 dye for 20 min. Next, the cells were washed with an incubation buffer two times. JC-1 could accumulate in functional mitochondria with high MMP and form JC-1 aggregates that emit red fluorescence, while dysfunctional mitochondrial with low MMP would release JC-1 monomers that emit green fluorescence. A fluorescence microscope was used to observe and image the rat NPMSCs. The ratio of green to red fluorescence intensity was calculated using the ImageJ software.

Mitochondrial reactive oxygen species analysis. MitoSOX green (Beyotime) was used to selectively estimate mitochondrial reactive oxygen species (ROS) levels following the manufacturer's instructions. The NPMSCs were seeded on a 24-well plate (5×10^4 cells/well), cultured at 37° overnight, and treated as the experimental design. Then, the rat NPMSCs were stained with MitoSOX green in the dark at 37° for 15 min and then washed with PBS three times. The ROS-specific fluorescence was assessed using a confocal microscope (Olympus, Tokyo, Japan). The mean fluorescent intensity of each group was normalized to that of the control group.

Senescence-associated β -Galactosidase staining. The senescence of cells was assessed using a Senescence β -Galactosidase (SA- β -Gal) staining Kit (Beyotime) according to the manufacturer's instructions. After indicated treatments, the cells were seeded onto a six-well plate (1×10^4 cells/well) and washed twice with PBS, followed by being fixed with fixation solution at room temperature for 15 min. Then, the cells were washed with PBS two times and incubated overnight with a freshly prepared staining solution at 37° in an incubator without CO₂. The SA- β -Gal-stained NPMSCs were observed using a light microscope and analyzed by ImageJ software. The blue-stained cells represented senescent NPMSCs.

Statistical analysis. All experiments were performed in at least three independent repeats. Statistical analysis was performed using GraphPad Prism 8 (GraphPad Software, San Diego, CA, USA). Data were described as the mean \pm standard deviation. One-way analysis of variance followed by Tukey's *post hoc* analysis and Student's *t*-test were used for comparative analyses. $P < 0.05$ was considered statistically significant.

Results

Identifications of rat NPMSCs

The MSC-associated surface markers were analyzed by flow cytometry. The isolated cells expressed high levels of CD73, CD90, and CD105 (MSC markers) and low levels of CD34, CD45, and HLA-DR (hematopoietic stem cell markers) (Fig. 1A). As Alizarin red staining revealed, the cells presented visible calcium deposits after osteogenic differentiation induction. After adipogenic differentiation, the oil droplets formed, as Oil Red O staining suggested (Fig. 1B). These

results suggest that the isolated rat NPMSCs meet the criteria of MSCs, as defined by ISCT.

Pretreatment with myricetin attenuates the H₂O₂-induced decrease in cell viability

The dose and time-response experiments were performed to choose an optimal concentration and time of myricetin and H₂O₂. The inhibitory effects of H₂O₂ on cell viability were most optimal at the dose of 100 μ M after 6 h of treatment. Therefore, in the subsequent experiments, the rat NPMSCs were treated with 100 μ M of H₂O₂ for 6 h (Fig. 2A). Additionally, 0–100 μ M of myricetin had no cytotoxicity to rat NPMSCs with different exposure times (0–24 h) (Fig. 2B). Moreover, pretreatment with 50 μ M myricetin for 24 h showed the maximum inhibitory effects on H₂O₂-induced decrease in cell viability (Fig. 2C). Therefore, we subsequently treated rat NPMSCs with 100 μ M of H₂O₂ for 6 h and 50 μ M myricetin for 24 h.

Myricetin at 50 μ M alleviates H₂O₂-induced cell apoptosis and mitochondrial dysfunction

As flow cytometry demonstrated, H₂O₂ significantly increased the apoptotic rate of rat NPMSCs, while myricetin abolished the H₂O₂-induced promotion in cell apoptosis. However, EX527 treatment reversed the inhibitory effects of myricetin on cell apoptosis (Fig. 3AB). The protein levels of cleaved caspase-3 and Bax were upregulated post-H₂O₂, while myricetin attenuated the H₂O₂-mediated increase in the protein levels of caspase-3 and Bax. However, after the EX527 treatment, the decreased protein levels were elevated. In parallel, the H₂O₂-induced inhibition in the protein level of Bcl-2 was rescued by myricetin, while EX527 attenuated the protective effects of myricetin, as western blotting showed (Fig. 3C). The reduction of MMP reflects mitochondrial dysfunction which is usually used for predicting early apoptosis. JC-1 is a specific fluorescent dye that accumulates in energized mitochondria. A significant MMP loss was found in the H₂O₂ group and myricetin treatment recovered the MMP loss (Fig. 3D, E). Moreover, the H₂O₂-induced increased mitochondrial ROS was decreased by myricetin, while EX527 limited the suppressive effect of myricetin on mitochondrial ROS production (Fig. 3F). Collectively, myricetin attenuates the H₂O₂-induced cell apoptosis and mitochondrial dysfunction, and EX527 treatment limits the protective effect of myricetin against H₂O₂-induced cell apoptosis and mitochondrial dysfunction.

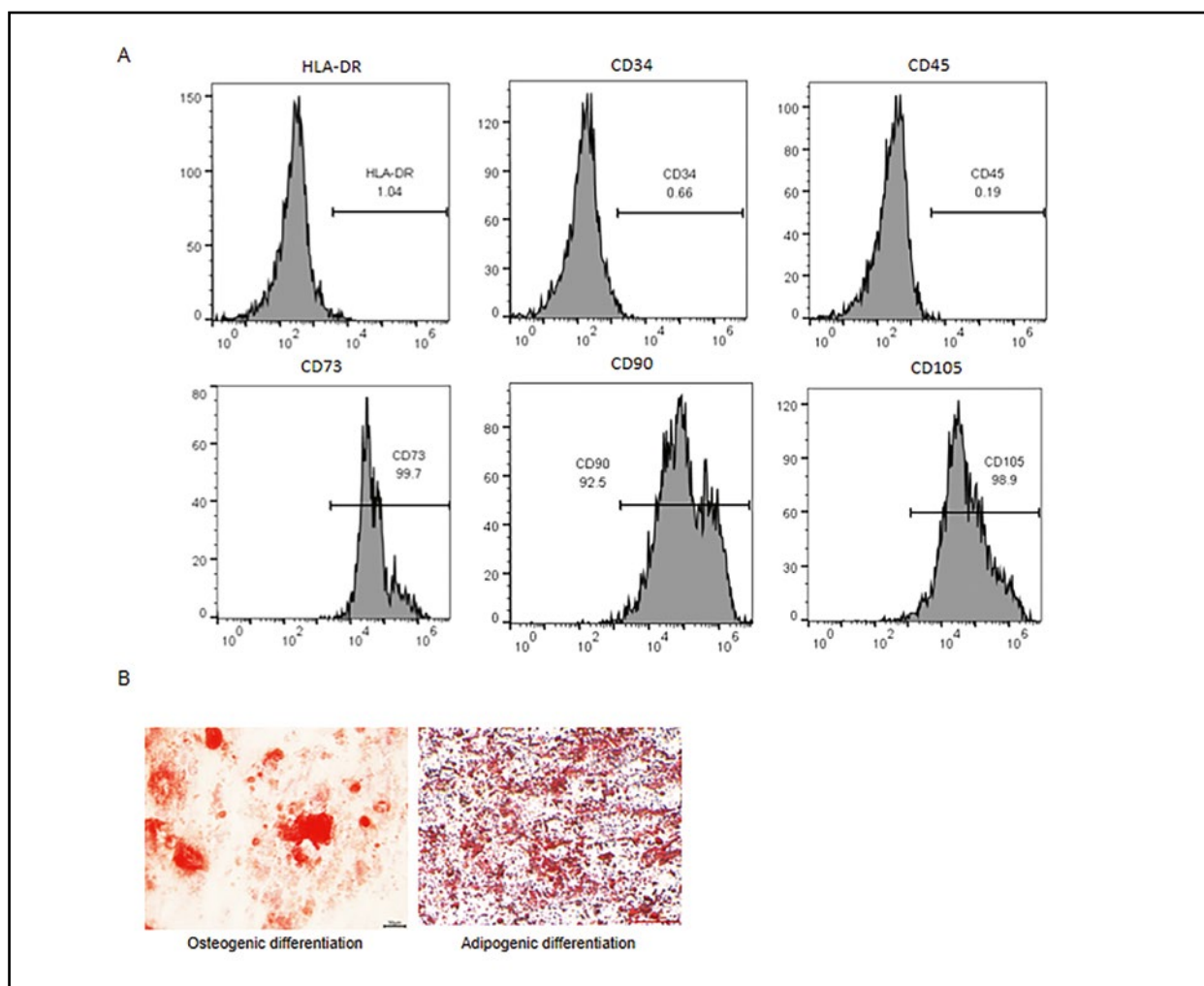


Figure 1. Identifications of rat nucleus pulposus derived mesenchymal stem cells (NPMSCs). **A.** The MSC-associated surface markers were detected on NPMSCs by flow cytometry as described in Methods. The x-axis means the signal intensity. The y-axis means cell counts. **B.** Osteogenic and adipogenic differentiation of NPMSCs were induced to examine the multilineage differentiation potential of rat NPMSCs as described in Methods. Then, the cells were stained with Alizarin red and Oil Red O, respectively, as described in Methods.

Myricetin at 50 μ M protects rat NPMSCs from senescence by affecting the SIRT1/PGC-1 α pathway

As SA- β -Gal staining revealed, H₂O₂ increased the number of SA- β -Gal-positive cells, while myricetin inhibited the promotion of the SA- β -Gal-positive rate induced by H₂O₂. However, EX527 reversed the inhibitory functions of myricetin on the number of SA- β -Gal-positive cells (Fig. 4A). The levels of senescence-associated proteins (p16, p21, p53) were upregulated following H₂O₂ treatment, while myricetin decreased their protein level. However, EX527 abolished the suppressive effects of myricetin (Fig. 4B). Finally, the decreased protein levels of SIRT1 and PGC-1 α induced by H₂O₂ were increased following myricetin treatment, while EX527 counteracted the enhancing effect of myricetin (Fig. 4C, D). Figure 5 presents the schematic diagram depicting the mecha-

nisms by which myricetin alleviates H₂O₂-induced senescence.

Discussion

Mesenchymal Stem Cells have been recognized as a novel therapeutic option for IVD regeneration [34]. However, limitations have been found to exist in the survival and adaptation of transplanted MSCs [35]. Myricetin at 50 μ M possesses antioxidant, anti-senescence, and anti-inflammatory activities [36, 37]. This study investigated the protective effects of myricetin (50 μ M) against senescence, apoptosis, and mitochondrial dysfunctions of rat NPMSCs.

H₂O₂ is one of the most common agents used to induce oxidative stress and damage cell biology by increasing intracellular ROS generation.

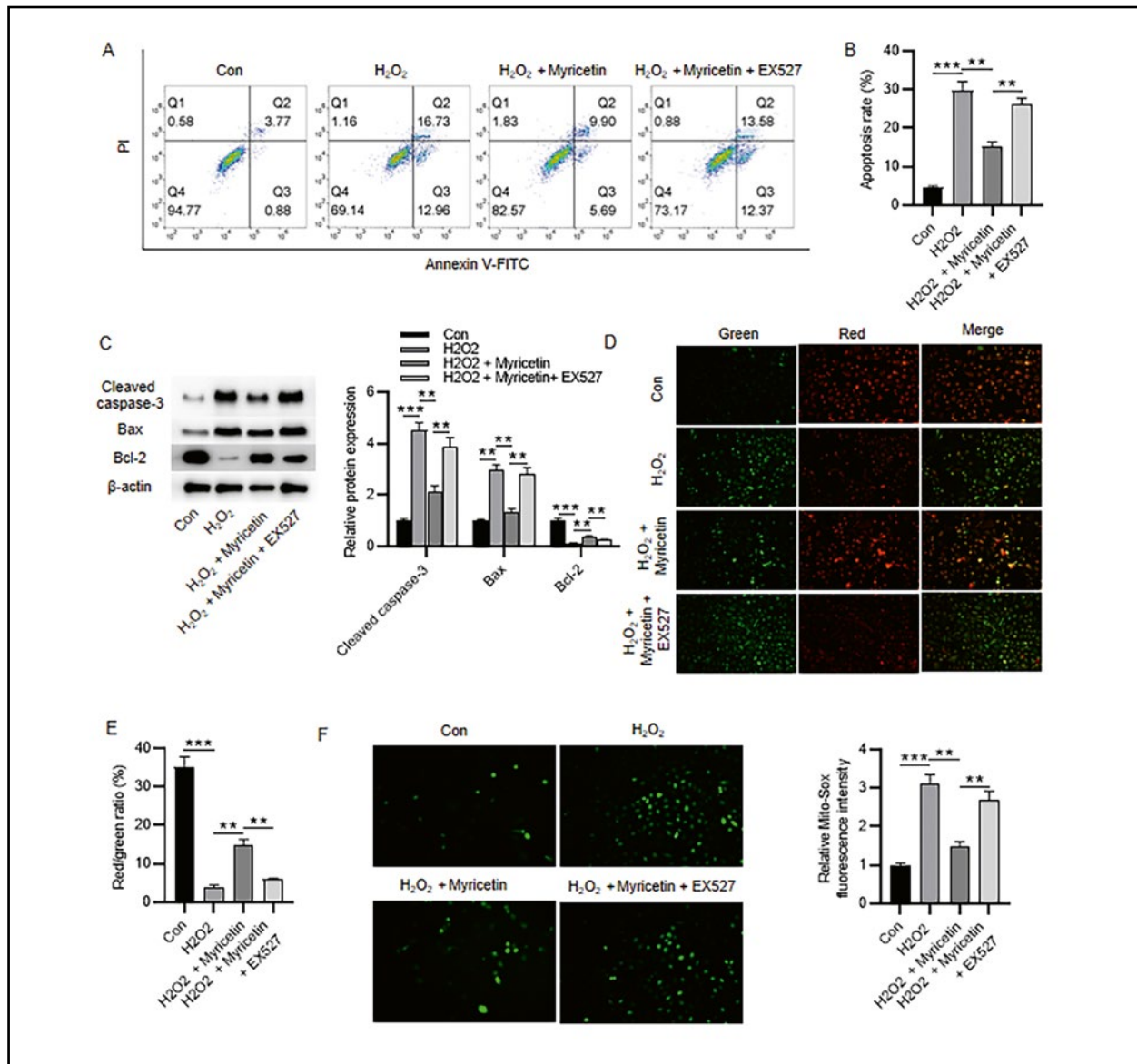


Figure 3. Myricetin at 50 μ M alleviates H₂O₂-induced cell apoptosis and mitochondrial dysfunction. **A–B.** Representative dot-plots and statistical analysis of NPMSC apoptosis rate by Annexin-V/PI staining in the control, the H₂O₂, the H₂O₂ + myricetin, and the H₂O₂ + EX527 (selective inhibitor of SIRT1) groups. The rat NPMSCs were pre-conditioned with 10 μ M EX527 prior to exposure to 100 μ M H₂O₂ for 6 h. **C.** The levels of apoptosis-associated proteins, Bax, Bcl-2, and cleaved caspase-3, were detected by western blotting. **D–E.** Fluorescence microscopy revealed mitochondrial membrane potential (MMP) changes after JC-1 staining of NPMSCs as described in Methods. **F.** The mitochondrial ROS levels in rat NPMSCs were examined by MitoSOX green staining as described in Methods. **P < 0.01, ***P < 0.001 vs. control cells.

In the current study, we found that H₂O₂ at the concentration of 100 μ M promoted intracellular ROS generation. This is in line with a previous study on NP cells [38], and indicates that excessive ROS generation may be responsible for H₂O₂-induced NPMSC apoptosis and mitochondrial dysfunction. Myricetin at 20 μ M attenuates the ROS production induced by arsenite and reduces the oxidative stress in natural killer cells [39]. Additionally, in bovine mammary epithelial cells, myricetin at 20 μ M significantly attenuates the

increase of ROS and MDA levels and alleviates the decrease of SOD and T-AOC levels induced by H₂O₂ by activating the AMPK/NRF2/ARE signaling [40]. Moreover, myricetin supplementation at two doses (25 and 50 mg/kg b.w.) demonstrated a protective effect in the colon of Wistar rats in cisplatin-induced toxicity by controlling oxidative stress and inflammation through normalizing the expression of both Nrf2 and NF- κ B [41]. In addition to oxidative stress, accumulating evidence has proven the protective effects of myricetin

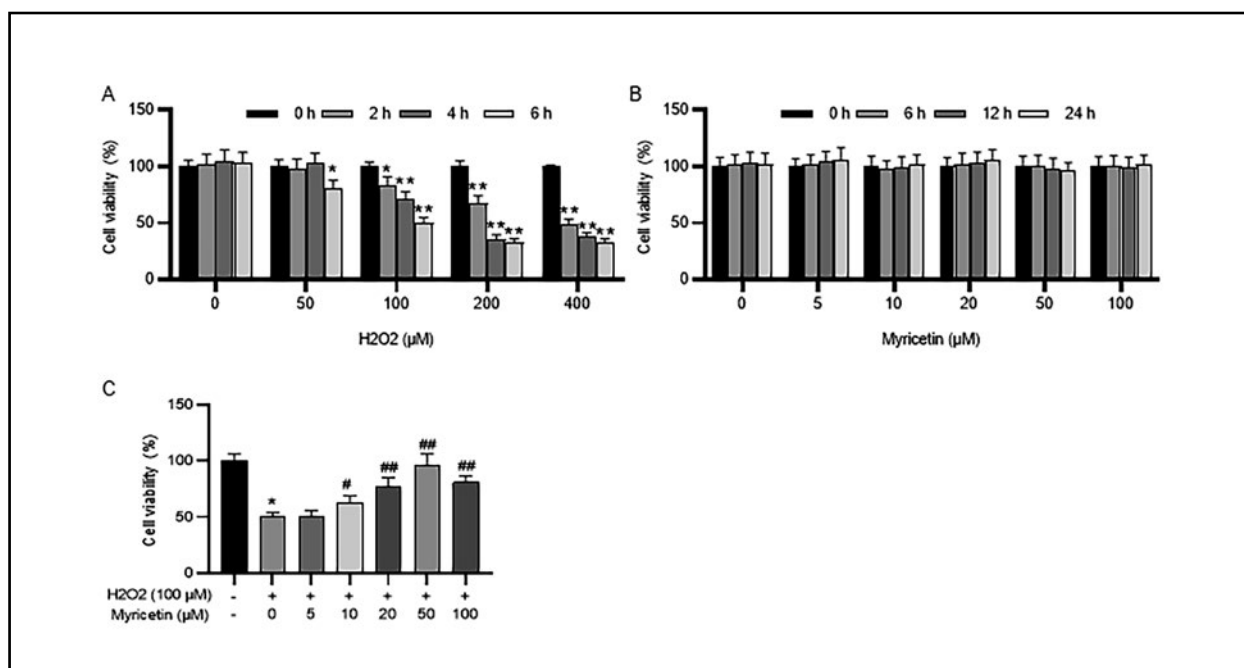


Figure 2. Pretreatment with myricetin attenuates the H₂O₂-induced decrease in cell viability of NPMSCs. The cells seeded onto 96-well plates (5×10^3 cells/well) were treated with 0–400 μM H₂O₂ for 0–6 h (A), with 0–100 μM myricetin for 0–24 h (B) and were pretreated with 0–100 μM myricetin for 24 h and then with 100 μM H₂O₂ for 6 h (C). The cell viability was measured by CCK-8 assay. All data are the means of \pm SEM in at least three independent experiments. For (A): * $P < 0.05$, ** $P < 0.01$ compared with control cells incubated for 0 h with H₂O₂. For (C) * $P < 0.05$ compared with H₂O₂ (0 μM) + myricetin (0 μM) group; # $P < 0.05$, ### $P < 0.01$ compared with H₂O₂ (100 μM) + myricetin (0 μM) group.

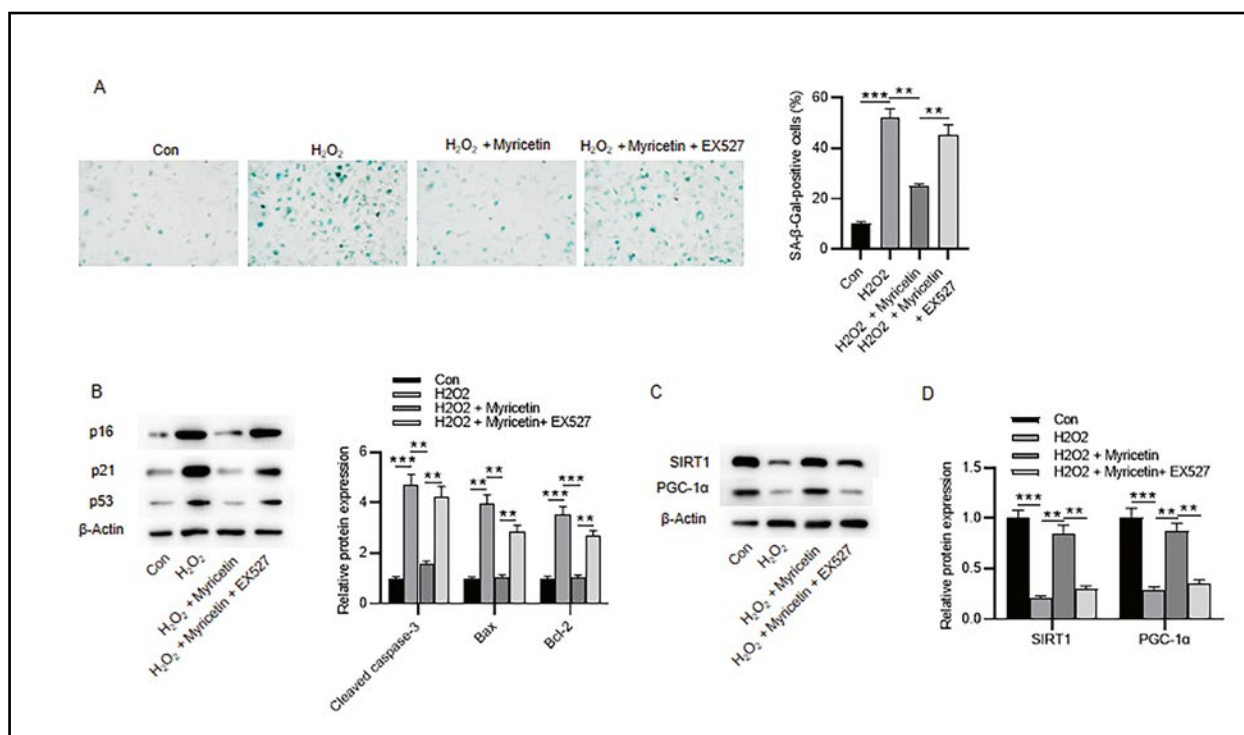


Figure 4. Myricetin at 50 μM reduces the expression of cell senescence markers in rat NPMSCs by affecting the SIRT1/PGC-1α pathway. **A.** Level of cell senescence was detected by SA-β-Gal staining. **B.** The levels of senescence-associated proteins (p16, p21, and p53) were detected by western blotting. **C–D.** NPMSCs treated with H₂O₂ for 6 h, NPMSCs pretreated with myricetin for 24 h prior to H₂O₂ treatment for 6 h, or NPMSCs pretreated with myricetin and EX527 for 24 h prior to H₂O₂ treatment for 6 h were used for western blotting analysis of SIRT1 and PGC-1α protein levels. The levels of proteins determined by western blotting were expressed in relation to the expression of β-actin. ** $P < 0.01$, *** $P < 0.001$.

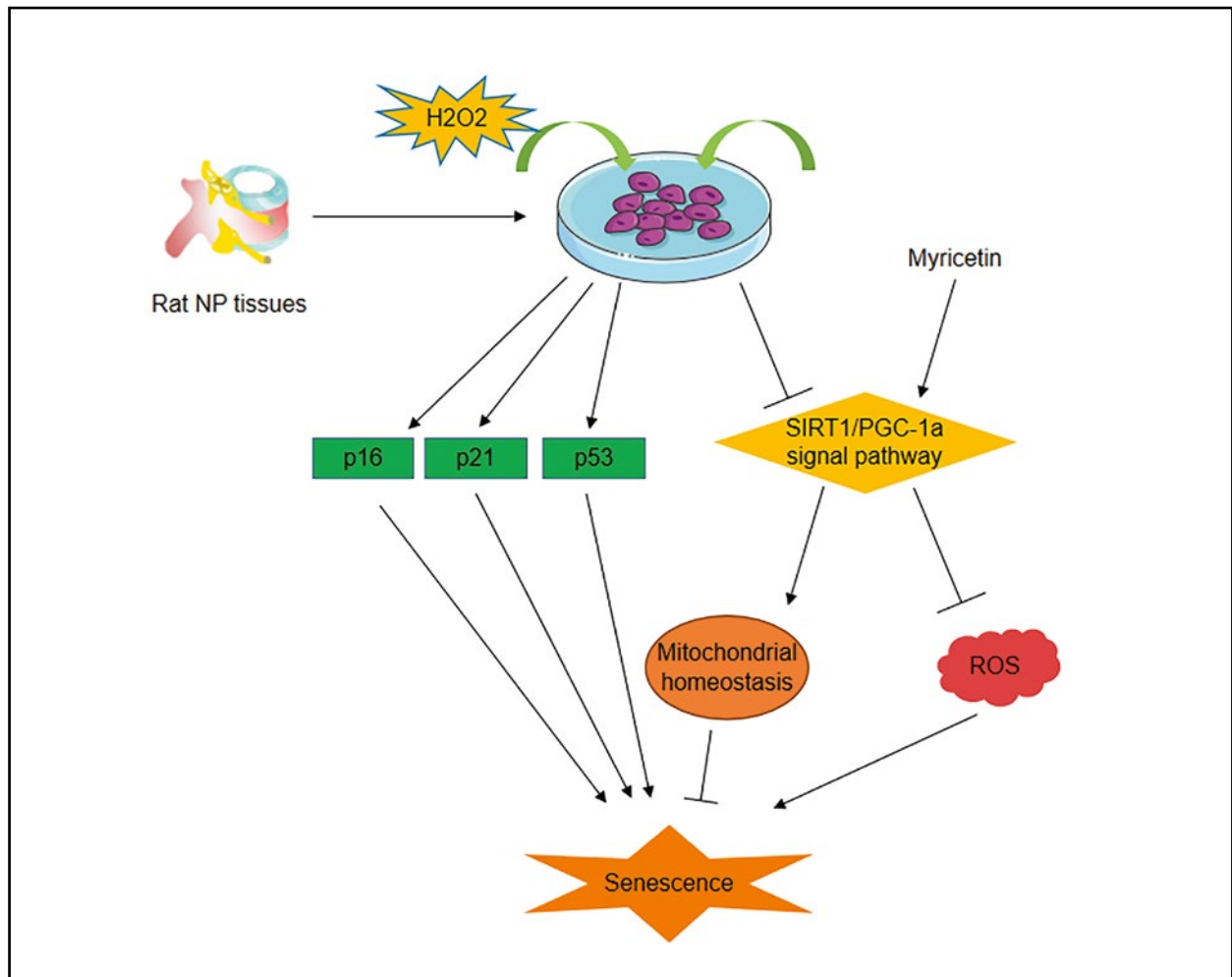


Figure 5. Schematic diagram depicting the mechanisms by which myricetin alleviates H₂O₂-induced senescence. Myricetin affects the SIRT1/PGC-1 α pathway to facilitate antioxidation, enhance mitochondrial homeostasis and alleviate rat NPMSC senescence *in vitro* which may delay intervertebral disc degeneration.

on mitochondrial function. For example, in skeletal muscles of hypoxia-exposed rats, pretreatment with myricetin at 50 μ M can restore mitochondrial dysfunctions by upregulating the AMPK and SIRT1 expression [42]. Additionally, myricetin at 40 and 80 μ M effectively reduces the aluminum phosphide-induced mitochondrial dysfunction in rat cardiomyocytes [43]. In the current study, we found that myricetin at 50 μ M abolished the H₂O₂-induced promotion in mitochondrial ROS production and limited the suppressive effect of H₂O₂ on mitochondrial membrane potential.

Nucleus pulposus-derived MSCs may differentiate into intervertebral discs cells and protect IVD cells from apoptosis, thus increasing the repair and regeneration ability of the degenerative IVDs [44]. It is crucial to maintain the number of viable and functional NPMSCs in the process of endogenous NPMSC repair [45]. As reported, myricetin possesses antiapoptotic properties. For example, myricetin

at 20 μ M exhibits protective effects against high glucose-induced apoptosis in INS-1 cells by attenuating endoplasmic reticulum stress and mitochondrial dysfunction [46]. Additionally, myricetin at 50 μ M was shown to alleviate the epoxiconazole-induced apoptosis in F98 glial cells by preventing ROS generation and DNA damage [47]. Moreover, myricetin at 5 μ M attenuates the low-density lipoprotein-induced apoptosis and ROS enhancement in human umbilical vein endothelial cells through the GAS5/miR-29a-3p//TLR4/NF- κ B pathway, clarifying a new mechanism of myricetin protection against atherosclerosis [48]. Here, we found that myricetin at 50 μ M alleviated the H₂O₂-induced apoptosis of rat NPMSCs, and this finding was confirmed by measuring the levels of apoptosis-associated proteins.

The generated ROS enhance the senescence and apoptosis of NP cells and NPMSCs, which are primary characteristics of IVDs [19, 49]. H₂O₂ at 100 μ M can

induce senescence of NPMSCs. Myricetin (25–100 μM) is suggested to reduce ROS-induced oxidative stress and downregulates senescence markers in glaucomatous trabecular meshwork cells [36]. In the current study, we found that myricetin at 50 μM alleviated the H_2O_2 -induced senescence of rat NPMSCs.

SIRT1/PGC-1 α activation attenuates oxidative damage and prevents metabolic disease, while SIRT1/PGC-1 α inactivation is involved in the pathomechanisms of mitochondrial disorders associated with xeroderma pigmentosum [50]. Myricetin at 60 μM was reported to increase SIRT1 activity to alleviate TNF- α -induced damage of A549 cells [51]. In the current study, we found that myricetin at 50 μM increased SIRT1 and PGC-1 α protein levels, and the inactivation of SIRT1/PGC-1 α pathway by the reversed the inhibitory effects of myricetin on cell apoptosis, cell senescence, and mitochondrial dysfunction.

In conclusion, this study reveals that myricetin at 50 μM attenuates the H_2O_2 -induced senescence and apoptosis in rat NPMSCs by affecting the SIRT1/PGC-1 α pathway.

However, there are limitations to our study. First, a previous study suggested that 50–100 μM H_2O_2 promoted the viability and proliferation of NPMSCs, and pretreatment with 75 μM H_2O_2 can better reduce oxidative stress and cell apoptosis in NPMSCs *in vitro* [52]. However, other studies have verified that H_2O_2 at 50–150 μM can lead to inhibition in the viability and proliferation of NPMSCs [53, 54]. Thus, the effect of H_2O_2 requires more investigation. Second, the elucidation of *in vivo* mechanisms of myricetin function needs further studies. Despite these limitations, we suggest that myricetin should be tested as an effective agent to improve the use of nucleus pulposus-derived MSCs in regenerative medicine.

Acknowledgments

The authors appreciate the help of the Wuhan Hospital of Traditional Chinese Medicine.

Conflict of interest

All authors declare no financial interests.

References

- Gianfredi V, Dinu M, Nucci D, et al. GBD 2017 Disease and Injury Incidence and Prevalence Collaborators. Global, regional, and national incidence, prevalence, and years lived with disability for 354 diseases and injuries for 195 countries and territories, 1990–2017: a systematic analysis for the Global Burden of Disease Study 2017. *Lancet*. 2018; 392(10159): 1789–1858, doi: [10.1016/S0140-6736\(18\)32279-7](https://doi.org/10.1016/S0140-6736(18)32279-7), indexed in Pubmed: 30496104.
- Dudek M, Yang N, Ruckshanthi JPD, et al. The intervertebral disc contains intrinsic circadian clocks that are regulated by age and cytokines and linked to degeneration. *Ann Rheum Dis*. 2017; 76(3): 576–584, doi: [10.1136/annrheumdis-2016-209428](https://doi.org/10.1136/annrheumdis-2016-209428), indexed in Pubmed: 27489225.
- Adams MA, Roughley PJ. What is intervertebral disc degeneration, and what causes it? *Spine (Phila Pa 1976)*. 2006; 31(18): 2151–2161, doi: [10.1097/01.brs.0000231761.73859.2c](https://doi.org/10.1097/01.brs.0000231761.73859.2c), indexed in Pubmed: 16915105.
- Cheung KMC, Karppinen J, Chan D, et al. Prevalence and pattern of lumbar magnetic resonance imaging changes in a population study of one thousand forty-three individuals. *Spine (Phila Pa 1976)*. 2009; 34(9): 934–940, doi: [10.1097/BRS.0b013e3181a01b3f](https://doi.org/10.1097/BRS.0b013e3181a01b3f), indexed in Pubmed: 19532001.
- Sclafani J, Leong M, Desai MJ, et al. Conventional versus high-frequency neuromodulation in the treatment of low back pain following spine surgery. *PM R*. 2019; 11(12): 1346–1353, doi: [10.1002/pmrj.12270](https://doi.org/10.1002/pmrj.12270), indexed in Pubmed: 31648418.
- Forozeshfard M, Jahan E, Amirsadat J, et al. Incidence and factors contributing to low back pain in the nonobstetrical patients operated under spinal anesthesia: a prospective 1-year follow-up study. *J Perianesth Nurs*. 2020; 35(1): 34–37, doi: [10.1016/j.jopan.2019.06.008](https://doi.org/10.1016/j.jopan.2019.06.008), indexed in Pubmed: 31635919.
- Roberts S, Evans H, Trivedi J, et al. Histology and pathology of the human intervertebral disc. *J Bone Joint Surg Am*. 2006; 88 Suppl 2: 10–14, doi: [10.2106/JBJS.F.00019](https://doi.org/10.2106/JBJS.F.00019), indexed in Pubmed: 16595436.
- Zhang F, Zhao X, Shen H, et al. Molecular mechanisms of cell death in intervertebral disc degeneration (Review). *Int J Mol Med*. 2016; 37(6): 1439–1448, doi: [10.3892/ijmm.2016.2573](https://doi.org/10.3892/ijmm.2016.2573), indexed in Pubmed: 27121482.
- Li Z, Peroglio M, Alini M, et al. Potential and limitations of intervertebral disc endogenous repair. *Curr Stem Cell Res Ther*. 2015; 10(4): 329–338, doi: [10.2174/1574888x10666150305105114](https://doi.org/10.2174/1574888x10666150305105114), indexed in Pubmed: 25741710.
- Beeravolu N, McKee C, Alamri A, et al. Isolation and characterization of mesenchymal stromal cells from human umbilical cord and fetal placenta. *J Vis Exp*. 2017(122), doi: [10.3791/55224](https://doi.org/10.3791/55224), indexed in Pubmed: 28447991.
- Guo Z, Su W, Zhou R, et al. Exosomal MATN3 of urine-derived stem cells ameliorates intervertebral disc degeneration by anti-senescence effects and promotes NPC proliferation and ECM synthesis by activating TGF-. *Oxid Med Cell Longev*. 2021; 2021: 5542241, doi: [10.1155/2021/5542241](https://doi.org/10.1155/2021/5542241), indexed in Pubmed: 34136064.
- Sun Y, Zhang W, Li Xu. Induced pluripotent stem cell-derived mesenchymal stem cells deliver exogenous miR-105-5p via small extracellular vesicles to rejuvenate senescent nucleus pulposus cells and attenuate intervertebral disc degeneration. , doi: [10.21203/rs.3.rs-127320/v1](https://doi.org/10.21203/rs.3.rs-127320/v1).
- Liao Z, Luo R, Li G, et al. Exosomes from mesenchymal stem cells modulate endoplasmic reticulum stress to protect against nucleus pulposus cell death and ameliorate intervertebral disc degeneration *in vivo*. *Theranostics*. 2019; 9(14): 4084–4100, doi: [10.7150/thno.33638](https://doi.org/10.7150/thno.33638), indexed in Pubmed: 31281533.
- Sakai D, Andersson GBJ. Stem cell therapy for intervertebral disc regeneration: obstacles and solutions. *Nat Rev Rheumatol*. 2015; 11(4): 243–256, doi: [10.1038/nrrheum.2015.13](https://doi.org/10.1038/nrrheum.2015.13), indexed in Pubmed: 25708497.
- Blanco JF, Graciani IF, Sanchez-Guijo FM, et al. Isolation and characterization of mesenchymal stromal cells from human degenerated nucleus pulposus: comparison with bone marrow mesenchymal stromal cells from the same subjects. *Spine (Phila Pa 1976)*. 2010; 35(26): 2259–2265, doi: [10.1097/BRS.0b013e3181cb8828](https://doi.org/10.1097/BRS.0b013e3181cb8828), indexed in Pubmed: 20622750.
- Li H, Tao Y, Liang C, et al. Influence of hypoxia in the intervertebral disc on the biological behaviors of rat adipose- and nucleus

- pulposus-derived mesenchymal stem cells. *Cells Tissues Organs*. 2013; 198(4): 266–277, doi: [10.1159/000356505](https://doi.org/10.1159/000356505), indexed in Pubmed: [24356285](https://pubmed.ncbi.nlm.nih.gov/24356285/).
17. Liu J, Tao H, Wang H, et al. Biological behavior of human nucleus pulposus mesenchymal stem cells in response to changes in the acidic environment during intervertebral disc degeneration. *Stem Cells Dev*. 2017; 26(12): 901–911, doi: [10.1089/scd.2016.0314](https://doi.org/10.1089/scd.2016.0314), indexed in Pubmed: [28298159](https://pubmed.ncbi.nlm.nih.gov/28298159/).
 18. Vadalà G, Ambrosio L, Russo F, et al. Interaction between mesenchymal stem cells and intervertebral disc microenvironment: from cell therapy to tissue engineering. *Stem Cells Int*. 2019; 2019: 2376172, doi: [10.1155/2019/2376172](https://doi.org/10.1155/2019/2376172), indexed in Pubmed: [32587618](https://pubmed.ncbi.nlm.nih.gov/32587618/).
 19. Feng C, Yang M, Lan M, et al. ROS: crucial intermediators in the pathogenesis of intervertebral disc degeneration. *Oxid Med Cell Longev*. 2017; 2017: 5601593, doi: [10.1155/2017/5601593](https://doi.org/10.1155/2017/5601593), indexed in Pubmed: [28392887](https://pubmed.ncbi.nlm.nih.gov/28392887/).
 20. Zorov DB, Juhaszova M, Sollott SJ. Mitochondrial reactive oxygen species (ROS) and ROS-induced ROS release. *Physiol Rev*. 2014; 94(3): 909–950, doi: [10.1152/physrev.00026.2013](https://doi.org/10.1152/physrev.00026.2013), indexed in Pubmed: [24987008](https://pubmed.ncbi.nlm.nih.gov/24987008/).
 21. Hu Y, Shao Z, Cai X, et al. Mitochondrial pathway is involved in advanced glycation end products-induced apoptosis of rabbit annulus fibrosus cells. *Spine (Phila Pa 1976)*. 2019; 44(10): E585–E595, doi: [10.1097/BRS.0000000000002930](https://doi.org/10.1097/BRS.0000000000002930), indexed in Pubmed: [30407277](https://pubmed.ncbi.nlm.nih.gov/30407277/).
 22. Shibata KR, Aoyama T, Shima Y, et al. Expression of the p16INK4A gene is associated closely with senescence of human mesenchymal stem cells and is potentially silenced by DNA methylation during in vitro expansion. *Stem Cells*. 2007; 25(9): 2371–2382, doi: [10.1634/stemcells.2007-0225](https://doi.org/10.1634/stemcells.2007-0225), indexed in Pubmed: [17569790](https://pubmed.ncbi.nlm.nih.gov/17569790/).
 23. Huang Y, Corbley MJ, Tang Z, et al. Down-regulation of p21WAF1 promotes apoptosis in senescent human fibroblasts: involvement of retinoblastoma protein phosphorylation and delay of cellular aging. *J Cell Physiol*. 2004; 201(3): 483–491, doi: [10.1002/jcp.20125](https://doi.org/10.1002/jcp.20125), indexed in Pubmed: [15389598](https://pubmed.ncbi.nlm.nih.gov/15389598/).
 24. Weng Z, Wang Y, Ouchi T, et al. Mesenchymal stem/stromal cell senescence: hallmarks, mechanisms, and combating strategies. *Stem Cells Transl Med*. 2022; 11(4): 356–371, doi: [10.1093/stclm/szac004](https://doi.org/10.1093/stclm/szac004), indexed in Pubmed: [35485439](https://pubmed.ncbi.nlm.nih.gov/35485439/).
 25. Tang BL. Sirt1 and the Mitochondria. *Mol Cells*. 2016; 39(2): 87–95, doi: [10.14348/molcells.2016.2318](https://doi.org/10.14348/molcells.2016.2318), indexed in Pubmed: [26831453](https://pubmed.ncbi.nlm.nih.gov/26831453/).
 26. Li J, Feng Li, Xing Y, et al. Radioprotective and antioxidant effect of resveratrol in hippocampus by activating Sirt1. *Int J Mol Sci*. 2014; 15(4): 5928–5939, doi: [10.3390/ijms15045928](https://doi.org/10.3390/ijms15045928), indexed in Pubmed: [24722566](https://pubmed.ncbi.nlm.nih.gov/24722566/).
 27. Liang D, Zhuo Y, Guo Z, et al. SIRT1/PGC-1 pathway activation triggers autophagy/mitophagy and attenuates oxidative damage in intestinal epithelial cells. *Biochimie*. 2020; 170: 10–20, doi: [10.1016/j.biochi.2019.12.001](https://doi.org/10.1016/j.biochi.2019.12.001), indexed in Pubmed: [31830513](https://pubmed.ncbi.nlm.nih.gov/31830513/).
 28. Kimura AM, Tsuji M, Yasumoto T, et al. Myricetin prevents high molecular weight Aβ oligomer-induced neurotoxicity through antioxidant effects in cell membranes and mitochondria. *Free Radic Biol Med*. 2021; 171: 232–244, doi: [10.1016/j.freeradbiomed.2021.05.019](https://doi.org/10.1016/j.freeradbiomed.2021.05.019), indexed in Pubmed: [34015458](https://pubmed.ncbi.nlm.nih.gov/34015458/).
 29. Yao X, Zhang J, Lu Y, et al. Myricetin restores Aβ-induced mitochondrial impairments in N2a-SW cells. *ACS Chem Neurosci*. 2022; 13(4): 454–463, doi: [10.1021/acscchemneuro.1c00591](https://doi.org/10.1021/acscchemneuro.1c00591), indexed in Pubmed: [35114083](https://pubmed.ncbi.nlm.nih.gov/35114083/).
 30. Jung HY, Lee D, Ryu HG, et al. Myricetin improves endurance capacity and mitochondrial density by activating SIRT1 and PGC-1α. *Sci Rep*. 2017; 7(1): 6237, doi: [10.1038/s41598-017-05303-2](https://doi.org/10.1038/s41598-017-05303-2), indexed in Pubmed: [28740165](https://pubmed.ncbi.nlm.nih.gov/28740165/).
 31. Chen S, Wu X, Lai Y, et al. Kindlin-2 inhibits Nlrp3 inflammasome activation in nucleus pulposus to maintain homeostasis of the intervertebral disc. *Bone Res*. 2022; 10(1): 5, doi: [10.1038/s41413-021-00179-5](https://doi.org/10.1038/s41413-021-00179-5), indexed in Pubmed: [35013104](https://pubmed.ncbi.nlm.nih.gov/35013104/).
 32. Huang Z, Cheng X, Zhao J, et al. Influence of simvastatin on the biological behavior of nucleus pulposus-derived mesenchymal stem cells. *Iran J Basic Med Sci*. 2019; 22(12): 1468–1475, doi: [10.22038/IJBMS.2019.14068](https://doi.org/10.22038/IJBMS.2019.14068), indexed in Pubmed: [32133066](https://pubmed.ncbi.nlm.nih.gov/32133066/).
 33. Ahn J, Kim MJ, Yoo A, et al. Identifying Codium fragile extract components and their effects on muscle weight and exercise endurance. *Food Chem*. 2021; 353: 129463, doi: [10.1016/j.foodchem.2021.129463](https://doi.org/10.1016/j.foodchem.2021.129463), indexed in Pubmed: [33743428](https://pubmed.ncbi.nlm.nih.gov/33743428/).
 34. Oehme D, Goldschlager T, Ghosh P, et al. Cell-based therapies used to treat lumbar degenerative disc disease: a systematic review of animal studies and human clinical trials. *Stem Cells Int*. 2015; 2015: 946031, doi: [10.1155/2015/946031](https://doi.org/10.1155/2015/946031), indexed in Pubmed: [26074979](https://pubmed.ncbi.nlm.nih.gov/26074979/).
 35. Migliorini F, Rath B, Tingart M, et al. Autogenic mesenchymal stem cells for intervertebral disc regeneration. *Int Orthop*. 2019; 43(4): 1027–1036, doi: [10.1007/s00264-018-4218-y](https://doi.org/10.1007/s00264-018-4218-y), indexed in Pubmed: [30415465](https://pubmed.ncbi.nlm.nih.gov/30415465/).
 36. Yang Q, Li Y, Luo L. Effect of myricetin on primary open-angle glaucoma. *Transl Neurosci*. 2018; 9: 132–141, doi: [10.1515/tnsci-2018-0020](https://doi.org/10.1515/tnsci-2018-0020), indexed in Pubmed: [30473883](https://pubmed.ncbi.nlm.nih.gov/30473883/).
 37. Ferreira LC, Grabe-Guimarães A, de Paula CA, et al. Anti-inflammatory and antinociceptive activities of campomanesia adamantium. *J Ethnopharmacol*. 2013; 145(1): 100–108, doi: [10.1016/j.jep.2012.10.037](https://doi.org/10.1016/j.jep.2012.10.037), indexed in Pubmed: [23123269](https://pubmed.ncbi.nlm.nih.gov/23123269/).
 38. Xu Y, Yao H, Wang Q, et al. Aquaporin-3 attenuates oxidative stress-induced nucleus pulposus cell apoptosis through regulating the P38 MAPK pathway. *Cell Physiol Biochem*. 2018; 50(5): 1687–1697, doi: [10.1159/000494788](https://doi.org/10.1159/000494788), indexed in Pubmed: [30384362](https://pubmed.ncbi.nlm.nih.gov/30384362/).
 39. Ma H, Song X, Huang P, et al. Myricetin protects natural killer cells from arsenite induced DNA damage by attenuating oxidative stress and retaining poly(ADP-Ribose) polymerase 1 activity. *Mutat Res Genet Toxicol Environ Mutagen*. 2021; 865: 503337, doi: [10.1016/j.mrgentox.2021.503337](https://doi.org/10.1016/j.mrgentox.2021.503337), indexed in Pubmed: [33865543](https://pubmed.ncbi.nlm.nih.gov/33865543/).
 40. Kan X, Liu J, Chen Y, et al. Myricetin protects against H2O2-induced oxidative damage and apoptosis in bovine mammary epithelial cells. *J Cell Physiol*. 2021; 236(4): 2684–2695, doi: [10.1002/jcp.30035](https://doi.org/10.1002/jcp.30035), indexed in Pubmed: [32885418](https://pubmed.ncbi.nlm.nih.gov/32885418/).
 41. Rehman MU, Rather IA. Myricetin abrogates cisplatin-induced oxidative stress, inflammatory response, and goblet cell disintegration in colon of wistar rats. *Plants (Basel)*. 2019; 9(1), doi: [10.3390/plants9010028](https://doi.org/10.3390/plants9010028), indexed in Pubmed: [31878169](https://pubmed.ncbi.nlm.nih.gov/31878169/).
 42. Zou D, Liu P, Chen Ka, et al. Protective effects of myricetin on acute hypoxia-induced exercise intolerance and mitochondrial impairments in rats. *PLoS One*. 2015; 10(4): e0124727, doi: [10.1371/journal.pone.0124727](https://doi.org/10.1371/journal.pone.0124727), indexed in Pubmed: [25919288](https://pubmed.ncbi.nlm.nih.gov/25919288/).
 43. Salimi A, Jamali Z, Shabani M. Antioxidant potential and inhibition of mitochondrial permeability transition pore by myricetin reduces aluminium phosphide-induced cytotoxicity and mitochondrial impairments. *Front Pharmacol*. 2021; 12: 719081, doi: [10.3389/fphar.2021.719081](https://doi.org/10.3389/fphar.2021.719081), indexed in Pubmed: [34858168](https://pubmed.ncbi.nlm.nih.gov/34858168/).
 44. Li XC, Wang MS, Liu W, et al. Co-culturing nucleus pulposus mesenchymal stem cells with notochordal cell-rich nucleus pulposus explants attenuates tumor necrosis factor-α-induced senescence. *Stem Cell Res Ther*. 2018; 9(1): 171, doi: [10.1186/s13287-018-0919-9](https://doi.org/10.1186/s13287-018-0919-9), indexed in Pubmed: [29941029](https://pubmed.ncbi.nlm.nih.gov/29941029/).
 45. Clouet J, Fusellier M, Camus A, et al. Intervertebral disc regeneration: From cell therapy to the development of novel bioinspired endogenous repair strategies. *Adv Drug Deliv Rev*. 2019; 146: 306–324, doi: [10.1016/j.addr.2018.04.017](https://doi.org/10.1016/j.addr.2018.04.017), indexed in Pubmed: [29705378](https://pubmed.ncbi.nlm.nih.gov/29705378/).

46. Karunakaran U, Elumalai S, Moon JS, et al. Myricetin protects against high glucose-induced β -Cell apoptosis by attenuating endoplasmic reticulum stress via inactivation of cyclin-dependent kinase 5. *Diabetes Metab J*. 2019; 43(2): 192–205, doi: 10.4093/dmj.2018.0052, indexed in Pubmed: 30688049.
47. Hamdi H, Abid-Essefi S, Eyer J. Neuroprotective effects of myricetin on epoxiconazole-induced toxicity in F98 cells. *Free Radic Biol Med*. 2021; 164: 154–163, doi: 10.1016/j.freeradbiomed.2020.12.451, indexed in Pubmed: 33429020.
48. Bai Y, Liu X, Chen Q, et al. Myricetin ameliorates ox-LDL-induced HUVECs apoptosis and inflammation via lncRNA GAS5 upregulating the expression of miR-29a-3p. *Sci Rep*. 2021; 11(1): 19637, doi: 10.1038/s41598-021-98916-7, indexed in Pubmed: 34608195.
49. Jiang LB, Cao L, Ma YQ, et al. TIGAR mediates the inhibitory role of hypoxia on ROS production and apoptosis in rat nucleus pulposus cells. *Osteoarthritis Cartilage*. 2018; 26(1): 138–148, doi: 10.1016/j.joca.2017.10.007, indexed in Pubmed: 29061494.
50. Fang EF, Scheibye-Knudsen M, Brace LE, et al. Defective mitophagy in XPA via PARP-1 hyperactivation and NAD(+)/SIRT1 reduction. *Cell*. 2014; 157(4): 882–896, doi: 10.1016/j.cell.2014.03.026, indexed in Pubmed: 24813611.
51. Chen M, Chen Z, Huang D, et al. Myricetin inhibits TNF- α -induced inflammation in A549 cells via the SIRT1/NF- κ B pathway. *Pulm Pharmacol Ther*. 2020; 65: 102000, doi: 10.1016/j.pupt.2021.102000, indexed in Pubmed: 33601000.
52. Zhang Yy, Hu Zl, Qi Yh, et al. Pretreatment of nucleus pulposus mesenchymal stem cells with appropriate concentration of H2O2 enhances their ability to treat intervertebral disc degeneration. *Stem Cell Research & Therapy*. 2022; 13(1), doi: 10.1186/s13287-022-03031-7.
53. Wang JW, Zhu L, Shi PZ, et al. 1,25(OH)2D3 mitigates oxidative stress-induced damage to nucleus pulposus-derived mesenchymal stem cells through PI3K/Akt pathway. *Oxid Med Cell Longev*. 2022; 2022: 1427110, doi: 10.1155/2022/1427110, indexed in Pubmed: 35340208.
54. Shi PZ, Wang JW, Wang PC, et al. Urolithin a alleviates oxidative stress-induced senescence in nucleus pulposus-derived mesenchymal stem cells through SIRT1/PGC-1 α pathway. *World J Stem Cells*. 2021; 13(12): 1928–1946, doi: 10.4252/wjsc.v13.i12.1928, indexed in Pubmed: 35069991.

Submitted: 16 February, 2023

Accepted after reviews: 22 May, 2023

Available as AoP: 29 May, 2023